Electronic Supplementary Material (ESI) for Physical Chemistry Chemical Physics.

Time-resolved Molecule Counting by Photon Statistics Across the Visible Spectrum

K. S. Grußmayer,*[ab] and D.-P. Herten*[a]

[a]Physikalisch-Chemisches Institut, Universität Heidelberg, Heidelberg, Germany, [b] École Polytechnique Fédérale de Lausanne, Laboratoire d'Optique Biomédicale, 1015 Lausanne, Switzerland

Counting by Photon Statistics (CoPS)

CoPS infers the number of independent fluorescent emitters (further referred to as emitter number) by analyzing the occurence of multiple photon detection events (mDE) in confocal microscopy.

In experiments, the sample typically consists of immobile, single probe molecules that sparsely decorate the surface. After generating an overview scan of the field of view, the photon statistics of each diffraction limited probe molecule is measured with pulsed laser excitation. A time correlated single-photon counting (TCSPC) unit records the individual photon arrival times for each of the four avalanche photodiodes (APDs) (for details on the instrumentation see Experimental and theoretical methods) of a modified Hanbury Brown-Twiss detection scheme. The laser pulses are short compared to the excited state lifetime with relatively long times between excitations, i.e. moderate laser repetition rates. This ensures that only single photons can be detected from a single fluorophore after one laser excitation pulse. The Monte-Carlo simulations mimic the experiments, but do not include simulation of the fluorescence lifetime of the emitters (for details see Experimental and theoretical methods).

The photon statistics thus carries information on the number of emitters in the excitation volume. The scheme in Figure S1a) illustrates the counting principle. If one emitter is present in the confocal volume, at most one photon can be detected. A single laser pulse can result in the detection of two or more photons only if two or more emitters are present. The frequency of up to four mDEs are reconstructed in data post-processing, as exemplified in Figure S1b for three different emitter numbers *N*.

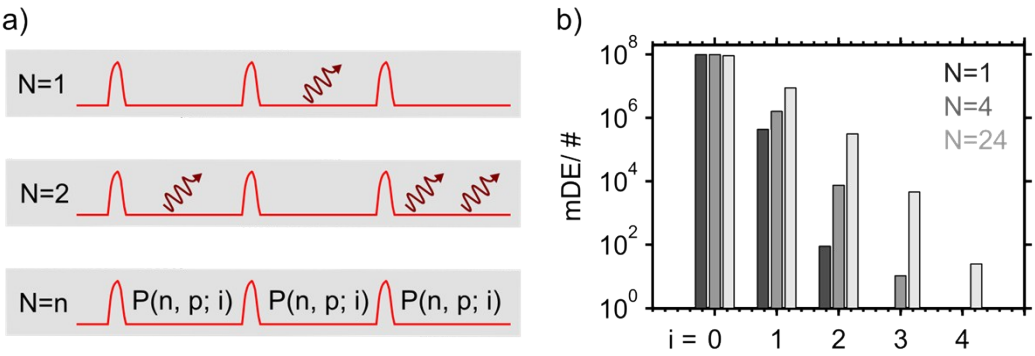

Figure S1. Counting by Photon Statistics. a) Scheme describing the probability of multiple photon detection events (mDE) after excitation with a pulsed laser for a certain number of independent emitters *N* in the laser focus. b) Expectation values for the relative frequencies for *i* detection events, i.e. the detection of *i* photons after a laser pulse, for *N* = 1, 4 and 24 emitters and four detectors (detection probability p = 0.4%, background detection probability p_b = 0.03%) for 10^8 simulated laser pulses.

For counting by photon statistics, the full mDE probabilities $P_m(N, p; i)$ are modeled (see eq S1 and S3-7 and Figure S1b). They depend on the number of emitters *N* and the average photon detection probability per laser pulse and per emitter (further referred to as detection probability) p of the microscope setup (see Equation S2). In the recursive expression, m denotes the number of detectors (here, m=4) while i is the number of multiple photons detected after one laser pulse. The model accounts for the stochastic processes of excitation, emission and detection of photons including the geometry of the detection path. Background photons in the photon probability distribution are modeled as an additional, fixed low detection probability of p_b. It

is important to note that the model takes into account that at most one photon can be detected by one APD after one laser pulse due to the dead time of the detectors and TCSPC electronics (~100ns). Background detection probabilities are typically estimated for each experiment and excitation laser power using the CoPS algorithm with p_b = 0 at the end of a trace when the fluorphores are photobleached. The resulting detection probabilities for estimated *N*=1 of 5–20 traces are averaged and used as input parameter p_b for the analysis. For simulations, the simulated p_b is used.

The number of emitters *N* and their detection probability *p* is estimated by non-linear regression with a Levenberg-Marquardt algorithm of the model $P_m(N, p; i)$ to the mDE histograms accumulated over the analysis period t_{acq}. Repeated subsampling of a randomly chosen subset of 75% of all laser cycles in the analysis period t_{acq} is used to achieve a more robust estimation. After 100 repetitions, the number of emitters for a single measurement is estimated as the median of the fit results and the error is indicated by the quantiles $Q_{0.25}$ and $Q_{0.75}$.

Modeling the photon probability distribution

The photon probability distribution P_m is given by

$$P_m(N,p;i)=\binom{m}{i}\left[\left(1-\binom{m-i}{m}p\right)^N\left(1-\binom{m-i}{m}p_b\right)\sum_{k\geq 0}\frac{\binom{i}{k}}{\binom{m}{k}}P_m(N,p;k)\right] \quad \text{(S1)}$$

with *N* the number of independent fluorescent emitters, *p* the detection probability (see eq S2), *m* the number of detectors, *i* the number of multiple detection events (mDE).

The detection probability *p* depends on the photon flux, i.e. the average laser intensity I_{laser} divided by the photon energy $h\nu$, the laser repetition frequency f_{rep}, the absorption cross-section σ_{abs}, the fluorescence quantum yield Q_f and the overall detection efficiency of the microscope setup *η*.

$$p=\frac{I_{laser}}{f_{rep}h\nu}\sigma_{abs}Q_f\eta=\frac{\varepsilon_{MB}}{f_{rep}} \quad \text{(S2)}$$

The molecular brightness ε_{MB} and the detection probability *p* are related by the laser repetition frequency. The photon probability distributions for the setup used in experiments with four detectors can be expressed explicitly as:

$$P_4(N,p;i=0)=(1-p)^N(1-p_b) \quad \text{(S3)}$$

$$P_4(N,p;i=1)=4\left(1-\frac{3}{4}p\right)^N\left(1-\frac{3}{4}p_b\right)-4(1-p)^N(1-p_b) \quad \text{(S4)}$$

$$P_4(N,p;i=2)=6\left(1-\frac{1}{2}p\right)^N\left(1-\frac{1}{2}p_b\right)-12\left(1-\frac{3}{4}p\right)^N\left(1-\frac{3}{4}p_b\right)+6(1-p)^N(1-p_b) \quad \text{(S5)}$$

$$P_4(N,p;i=3)=4\left(1-\frac{1}{4}p\right)^N\left(1-\frac{1}{4}p_b\right)-12\left(1-\frac{1}{2}p\right)^N\left(1-\frac{1}{2}p_b\right)+12\left(1-\frac{3}{4}p\right)^N\left(1-\frac{3}{4}p_b\right)-4(1-p)^N(1-p_b) \quad \text{(S6)}$$

$$P_4(N,p;i=4)=1-4\left(1-\frac{1}{4}p\right)^N\left(1-\frac{1}{4}p_b\right)+6\left(1-\frac{1}{2}p\right)^N\left(1-\frac{1}{2}p_b\right)-4\left(1-\frac{3}{4}p\right)^N\left(1-\frac{3}{4}p_b\right)-(1-p)^N(1-p_b) \quad \text{(S7)}$$

In fact, the probability to detect *i* photons per laser cycle for a given emitter number scales with p^i:[13]

$$P_4(N,p;1\leq i\leq 4)\sim\prod_{k=0}^{i-1}(N-k)\,p^i \; for\; small\; Np\ll 1 \quad \text{(S8)}$$

Filter sets and lasers

Table S1. Filters and lasers used for experiments. All filters are from AHF Analysetechnik (Tübingen, Germany) and all lasers are from PicoQuant (Berlin, Germany).

Experiment	Laser and Notch Filter	Dichroic Mirror	Bandpass Filter	Shortpass Filter
640 nm excitation [a]	LDH-P-C-640B, triple notch	Dual Line Strahlenteiler	ET Bandpass	-

	filter 488/532/631-640	zt532/640rpc	685/70	
635 nm excitation[b]	fibre coupled, randomly polarized LDH-P-635 with cleanup filter HQ 635/10, dual notch filter 488/635	Dual Line Strahlenteiler z488/633	ET Bandpass 685/70	-
532 nm excitation[c]	532nm Pico TA, triple notch filter 488/532/631-640	Strahlenteiler 530dcxr,	BrightLine 582/75	694/SP HC Kurzpass-Filter BrightLine
470 nm excitation[d]	LDH-P-C-470 with cleanup filter z473/10, single notch filter zet473NF	HC Laser-Strahlenteiler BS R488	Laser-Sperrfilter HQ 530/60	-
470 nm excitation II[e]	LDH-P-C-470 with cleanup filter z473/10, single notch filter zet473NF	HC Laser-Strahlenteiler BS R488	-	694/SP HC Kurzpass-Filter BrightLine

[a] tetraAtto633/647N and DNA hybridization sample with Silicon Rhodamine, [b]DNA hybridization sample with Atto647N, Atto633, Cy5, Alexa647 and AbberiorStar635 and streptavidin-Alexa647, [c]DNA hybridization sample with Cy3B, Atto565, Atto550, AttoRho6G, Atto532 and Alexa532, [d]DNA hybridization sample with OregonGreen514, OregonGreen488, Atto488 and Alexa488, [e].conjugated polymer poly(3-hexylthiophene).

Properties of the DNA probes

The properties of the DNA hybridization probes with 635 nm excitation are listed in Grussmayer et al. [1].

Table S2. Degree of labeling (DOL) of DNA probes with different fluorophores and 640 nm excitation measured by ensemble absorption spectroscopy and number of probes *n* measured in single molecule experiments.

	tetraAtto633	tetraAtto647N	SiR hybridization probe
DOL REP_4' or REP'	3.8 ± 0.8	3.7 ± 0.7	1.4 ± 0.3
DOL REP_4	-	-	-
n/ #	2.5µW/5µW/10µW/20µW 97/91/152/164	20µW 143	5µW/10µW 157/ 154

Table S3. Degree of labeling (DOL) of DNA hybridization probe with different fluorophores and 532 nm excitation measured by ensemble absorption spectroscopy and number of probes *n* measured in single molecule experiments.

	Cy3B	Atto550	Atto565	AttoRho6G	Alexa532	Atto532
DOL REP'	1.84 ± 0.4	1 ± 0.2	0.85 ± 0.2	0.91 ± 0.2	1.53 ± 0.3	0.99 ± 0.2
DOL REP_4	-	-	-	-	-	-
n/ # high/low laser power	127/ 123	149/ 156	149/ 198	130/ 107	148/ -	150/ -

Table S4. Degree of labeling (DOL) of DNA hybridization probe with different fluorophores and 470 nm excitation measured by ensemble absorption and number of probes *n* measured in single molecule experiments.

	Atto488	Alexa488	OregonGreen488	OregonGreen514

DOL REP'	1.0 ± 0.2	1.2 ± 0.2	0.8 ± 0.2	1.1 ± 0.2
DOL REP_4	-	0.75±0.2	-	-
n/ #	233	176	225	159

Table S5. Fluorescence properties and brightness comparison of fluorophores with 635 nm/640 nm laser excitation. Table S1 of Grussmayer et al.[1] modified.

	Atto647N	Atto633	Cy5	Alexa647	AbberiorStar635	SiR
λ_{abs}/ nm	644	629	649	650	634	652
λ_{em}/ nm	669	657	670	665	654	674
$\varepsilon_{max}/10^5 M^{-1}$ cm^{-1}	1.5	1.3	2.5	2.39	0.6	1,0
$\varepsilon_{635\ nm}/10^5 M^{-1}$ cm^{-1}	1.15	1.21	2.1	1.5	0.57	0.74
Q_f	0.65	0.64	>0.28	0.33	0.51	0.39
B = $\varepsilon_{635\ nm}Q_f/10^5 M^{-1}$ cm^{-1}	0.75	0.77	>0.58	0.49	0.29	0.28

Table S6. Fluorescence properties and brightness comparison of fluorophores with 532 nm laser excitation.

	Cy3B	Atto550	Atto565	AttoRho6G	Alexa532	Atto532
λ_{abs}/ nm	559	554	563	535	532	532
λ_{em}/ nm	570	576	592	560	554	553
$\varepsilon_{max}/10^5 M^{-1}$ cm^{-1}	1.3	1.2	1.2	1.15	0.81	1.15
$\varepsilon_{635\ nm}/10^5 M^{-1}$ cm^{-1}	0.78	0.48	0.46	1.13	0.81	1.15
Q_f	>0.67	0.8	0.9	0.9	0.61	0.9
B = $\varepsilon_{635\ nm}Q_f/10^5 M^{-1}$ cm^{-1}	>0.52	0.38	0.41	1.02	0.49	1.04

Table S7. Fluorescence properties and brightness comparison of fluorophores with 470 nm laser excitation.

	Atto488	Alexa488	OregonGreen488 (6-Isomer)	OregonGreen514
λ_{abs}/ nm	501	495	495	506
λ_{em}/ nm	523	519	516	526
$\varepsilon_{max}/10^5 M^{-1}$ cm^{-1}	0.9	0.71	0.82	0.85
$\varepsilon_{635\ nm}/10^5 M^{-1}$ cm^{-1}	0.33	0.33	0.35	0.22
Q_f	0.8	0.92	0.92	-
B = $\varepsilon_{635\ nm}Q_f/10^5 M^{-1}$ cm^{-1}	0.26	0.30	0.32	-

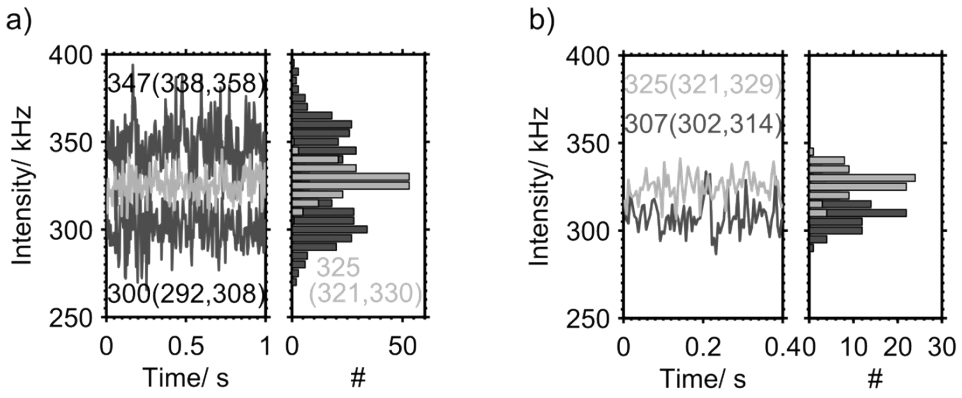

Figure S2. Comparison of experiments with simulation. Graphs display the intensity over time and the intensity histogram along with its quantiles (median($Q_{0.25}$,$Q_{0.75}$)). Simulation with N = 4, p = 0.4% and p_b = 0.03% (light grey) and experiments with the tetraAtto633 probe at 10 µW laser excitation power at 640 nm and a laser repetition rate of 20 MHz (dark grey). Experimental traces with higher (a)) and comparable (b)) intensity fluctuation than the simulated trace.

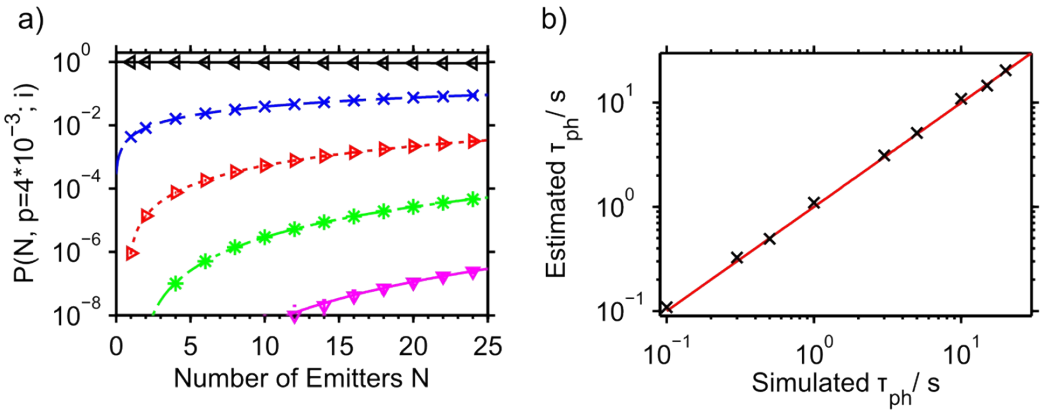

Figure S3. Verification of simulations. a) Comparison of the probability for mDE from data with 10^8 simulated laser pulses (symbols indicate the median of 200 simulated traces with the lower and upper quartiles as error bars; the error is very small and cannot be seen) and of the CoPS model supplied with simulation parameters detection probability p = 0.4%, background detection probability p_b = 0.03% (lines). Black left-pointing triangles i = 0, blue crosses i = 1, red right-pointing triangles i = 2, green asterisks i = 3, magenta downward-pointing triangle i = 4. b) Comparison of the average photostability times τ_{ph} (black crosses) estimated by fitting the sum of 200 simulated intensity traces with a monoexponential decay and the simulated τ_{ph} parameters. The red line indicates the true, simulated photostability times.

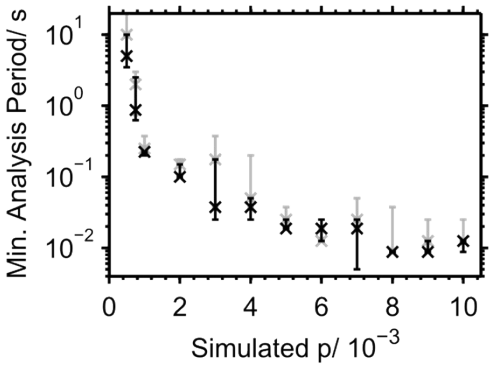

Figure S4. Comparison of minimum analysis period determined by different criteria. Minimum analysis period shown for varying simulated detection probability determined by the relative deviation from the maximum obtained emitter number estimate (black) and determined by a deviation of 5% or less from the simulated emitter number (grey). The error bars are derived by varying the threshold to determine the minimum analysis period to 90% and 95% of the maximum moving average, respectively.

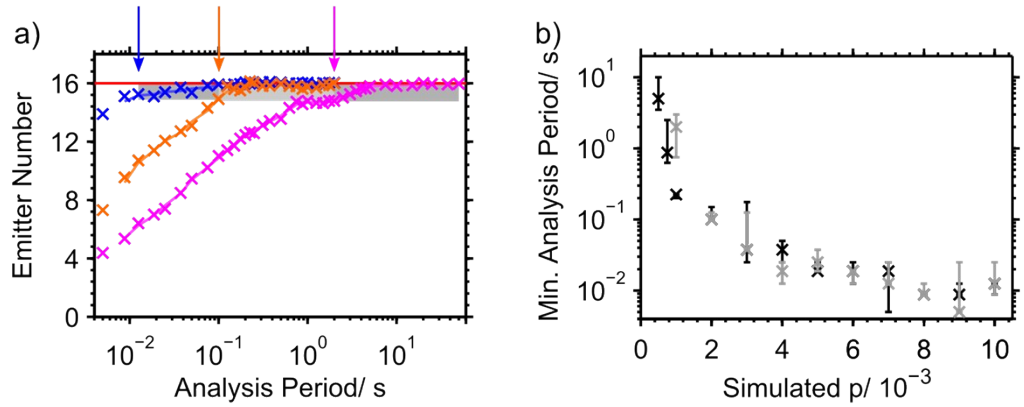

Figure S5. Comparison of minimum analysis period for simulations and photon statistics analysis with N = 4 emitters and N = 16 emitters. a) Median of estimated emitter numbers for CoPS analysis with varying analysis period in blue/orange/magenta for simulated N = 16, p = (10/2/1)x10^{-3} and p_b = (6/2/1)x10^{-4}. The blue/orange/magenta line is the three point moving average of emitter number estimates and the plateau of valid CoPS estimates is shaded in dark grey/light grey. The red line indicates the simulated emitter number N = 16. b) Minimum analysis period for simulated detection probability p = (10/9/8/7/6/5/4/3/2/1/0.75/0.5)x10^{-3} and p_b = (6/5.5/5/4.5/4/3.5/3/2.5/2/1/0.75/0.5)x10^{-4} for N = 4 (black) and N = 16 (grey).

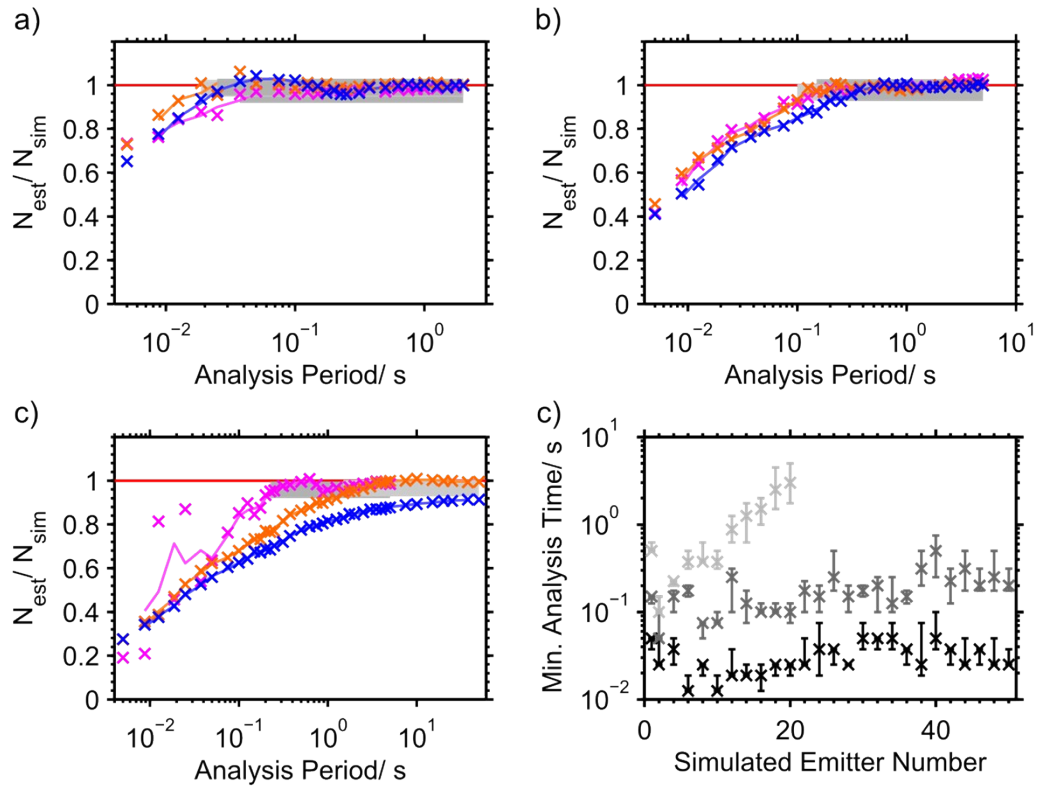

Figure S6. Comparison of minimum analysis period for simulations and photon statistics analysis with N = 1, 2, 4, …50 emitters and different detection probabilities. Median of estimated emitter numbers for CoPS analysis with varying analysis period in blue/orange/magenta for simulated a) N = 4/16/50, p = 4x10^{-3} and p_b = 3x10^{-4}, b) N = 4/16/50, p = 2x10^{-3} and p_b = 2x10^{-4}, c) N = 4/16/28, p = 1 10^{-3} and p_b = 1x10^{-4}. The blue/orange/magenta line is the three point moving average of emitter number estimates and the plateau of valid CoPS estimates is shaded in dark grey/light grey. The red line indicates the normalized simulated emitter number. d) Minimum analysis period for simulated detection probability p = (4/2/1)x10^{-3} (black/dark grey/light grey).

Connecting the minimum photostability with Fluorophore brightness

For simplicity, we assume that the timepoints of fluorophore photobleaching are distributed according to a monoexponential probability distribution function *pdf(t, τ_{ph})* given in eq S9. The probability for fluorophores to photobleach in a certain timespan Δt is then given by the cumulative distribution function *cdf(*Δ*t, τ_{ph})* (see eq S10). In turn, the probability for fluorophores to still be fluorescent after Δ*t* is P_{ph}*(*Δ*t, τ_{ph})* = 1 - *cdf(*Δ*t, τ_{ph})* (see eq S11). Photobleaching of a pure N-mer leads to a distribution of label numbers k that can be described by a binomial distribution with fluorescence 'success' probability P_{ph}*(*Δ*t, τ_{ph})*. The average of the binomial distribution is NP_{ph}, thus the fraction of molecules that are still fluorescent after a certain analysis period t_{acq} is given by eq S12 and this fraction of surviving fluorophores is plotted in Figure S7 for typical parameters.

$$pdf(t;\tau_{ph}) = \frac{1}{\tau_{ph}} e^{-\frac{t}{\tau_{ph}}} \tag{S9}$$

$$cdf(\Delta t;\tau_{ph}) = \int_0^{\Delta t} pdf(t;\tau_{ph})dt = 1 - e^{-\frac{\Delta t}{\tau_{ph}}} \tag{S10}$$

$$P_{ph}(\Delta t;\tau_{ph}) = 1 - cdf(\Delta t;\tau_{ph}) = e^{-\frac{\Delta t}{\tau_{ph}}} \tag{S11}$$

$$F_{surv}(t_{acq},\tau_{ph}) = \frac{\langle k\rangle(t_{acq},\tau_{ph})}{N} = P_{ph}(t_{acq};\tau_{ph}) = e^{-\frac{t_{acq}}{\tau_{ph}}} \tag{S12}$$

We can now estimate the minimum required photostability necessary to retain a certain fraction of surviving molecules for fluorophores of a particular brightness by using the minimum analysis period that delivers valid CoPS estimates determined by simulations with different detection probabilities as a starting point:

$$\tau_{ph,min}(t_{acq,min}(p), F_{surv}) = -\frac{t_{acq,min}(p)}{ln(F_{surv})} \quad \text{(S13)}$$

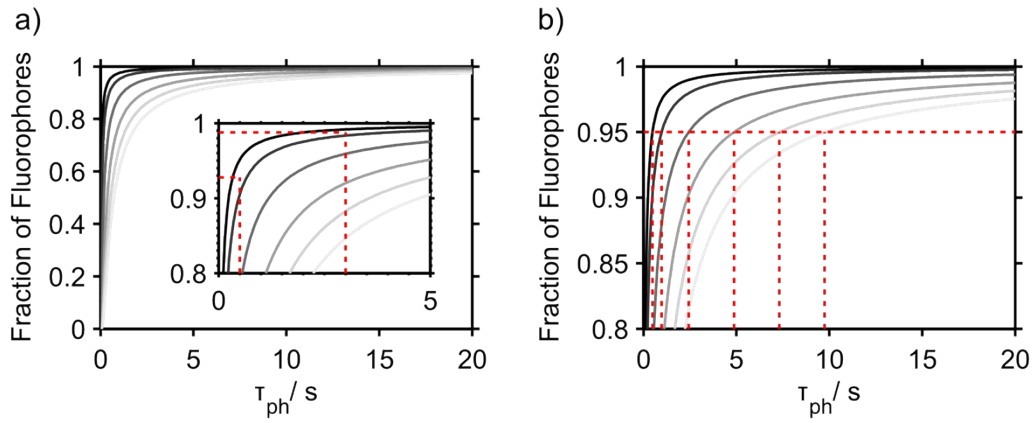

Figure S7. Modeling the fraction of surviving fluorophores. a) Fraction of remaining fluorescent labels for certain analysis periods with varying average photostability time. t_{acq} = 25/50/125 /250/375/500 ms from dark grey to light grey. The dotted red line indicates the fraction of remaining fluorescence for τ_{ph} = 0.5 s and τ_{ph} = 3 s. b) Same as a). The dotted red lines indicates the average photobleaching time τ_{ph} corresponding to 95% remaining fluorescence for the set of curves.

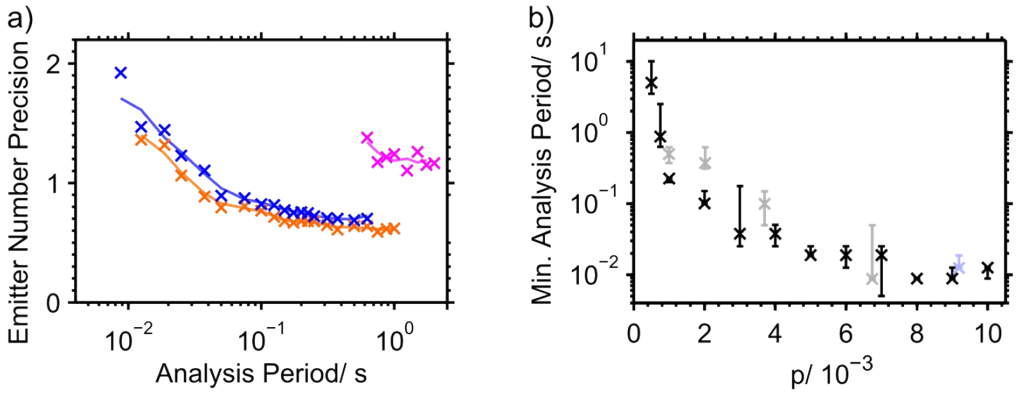

Figure S8. Experiments and photon statistics analysis with tetraProbes and varying laser excitation power. a) Precision of estimated emitter numbers for CoPS analysis with varying analysis period in magenta/blue for tetraAtto633 with 2.5 µW/20 µW laser excitation power and in orange for tetraAtto647N with 20 µW at 640 nm and a repetition rate of 20 MHz. The blue/orange/magenta line is the three point moving average. B) Comparison of minimum analysis periods for varying detection probability in simulations (black) with minimum analysis periods in experiments. TetraAtto633 measurements with 2.5 µW/5 µW/10 µW and 20 µW (grey) and tetraAtto647N measurements (light blue) with 20 µW laser excitation power at 640nm and a repetition rate of 20 MHz. The error bars are derived by varying the threshold to determine the minimum analysis period to 90% and 95% of the maximum moving average, respectively.

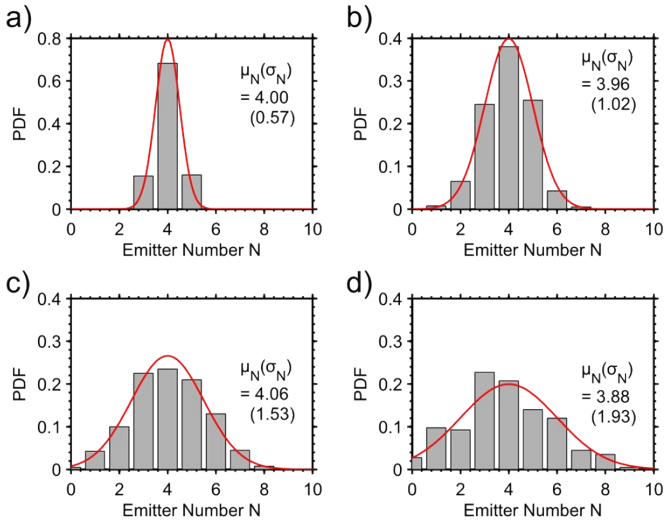

Figure S9. Exemplary verification of simulations with variable number of emitters. Probability distribution functions (PDF) for the number of simulated emitters (grey bars) together with the average (standard deviation) and the PDF of a Gaussian (red line) supplied with the simulation parameters $\mu_{N,\,sim}$ = 4.0 and $\sigma_{N,\,sim}$ = 0.5/1.0/1.5/2.0 in a)/b)/c)/d). Additional simulation parameters: detection probability p = 0.4%, background detection probability p_b = 0.03% and 400 simulated traces.

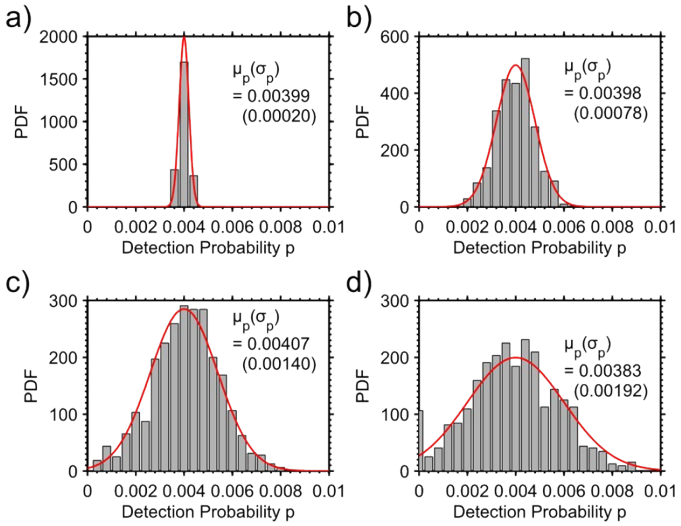

Figure S10. Exemplary verification of simulations with variable detection probability. Probability distribution functions (PDF) for the simulated detection probability (grey bars) together with the average (standard deviation) and the PDF of a Gaussian (red line) supplied with the simulation parameters $\mu_{p,\,sim}$ = 0.4% and $\sigma_{p,\,sim}$ = (0.02//0.08/0.14/0.2)% in a)/b)/c)/d). Additional simulation parameters: emitter number N = 4, background detection probability p_b = 0.03% and 200 simulated traces.

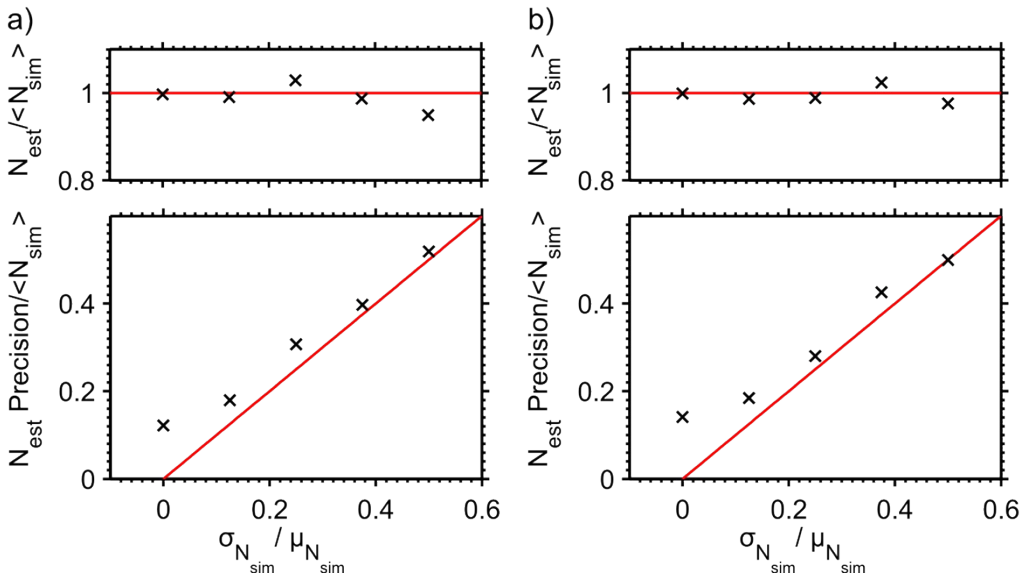

Figure S11. Simulations with variable number of emitters. Simulated mean emitter number a) $\mu_{N,\,sim}$ = 4.0 and b) $\mu_{N,\,sim}$ = 16.0 with increasing variability. Median estimated emitter number (top) and estimated emitter number precision (bottom) for t_{acq} = 500 ms relative to the mean of the simulated emitter numbers as a function of increasing $\sigma_{N,\,sim}$ relative to $\mu_{N,\,sim}$. The red line indicates the target relative emitter number (top) and the bisecting line (bottom). Additional simulation parameters: detection probability p = 0.4%, background detection probability p_b = 0.03% and 400 simulated traces.

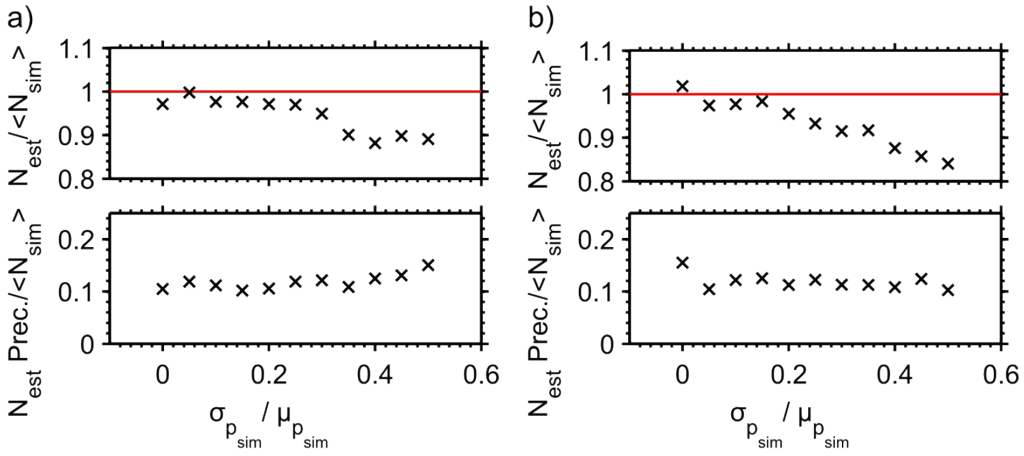

Figure S12. Simulations with variable photon detection probability. Simulated emitter number a) N = 4 and b) N = 16 with increasing variability of the detection probability. Median estimated emitter number (top) and estimated emitter number precision (bottom) for t_{acq} = 500 ms relative to the mean of the simulated emitter numbers as a function of increasing $\sigma_{p,\,sim}$ relative to $\mu_{p,\,sim}$. The red line indicates the target relative emitter number (top). Additional simulation parameters: detection probability $\mu_{p,\,sim}$ = 0.4%, background detection probability p_b = 0.03% and 200 simulated traces.

Photostability and control of photophysics for DNA hybridization probes

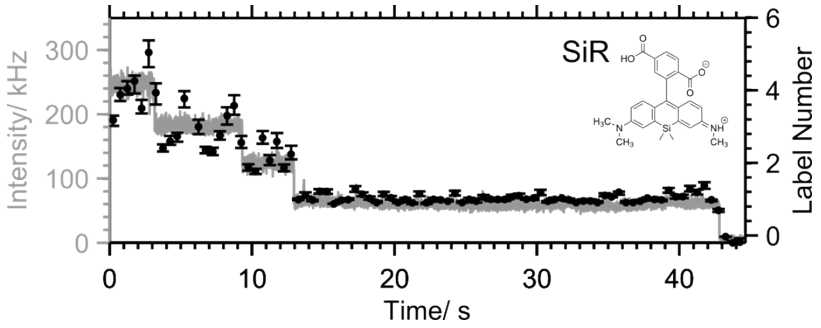

Figure S13. Single molecule CoPS analysis of DNA hybridization probe labeled with SiR. 10 µW laser excitation power at 640 nm and a repetition rate of 20 MHz. Time resolution (= analysis period t_{acq}) of 500 ms. CoPS estimates correlate with intensity bleaching steps. Label number estimates with error bars derived from resampling algorithm (black), intensity (grey).

All buffers achieved photostabilization compared to imaging of the dyes in PBS (TIRF and confocal experiments, data not shown). Atto647N, Atto633, Cy5, Alexa647 and AbberiorStar635 from [1], SiR, Cy3B and Alexa532 were nicely stabilized except for rare, long off-times (seconds timescale). Atto550 and Atto565 displayed almost no fast blinking (millisecond off-time), but frequently entered a dimmer fluorescent states with time, which rendered identification of photobleaching steps difficult. For AttoRho6G fast blinking was not completely prevented, but the dye showed no other fluctuations in fluorescence intensity. Atto532 often presented residual, dim fluorescence at the end of intensity traces. For the dyes that were excited with a 470 nm laser, photobleaching was prominent.

Figure S14 (following page). Single molecule CoPS analysis of DNA hybridization probe with dyes that are excited with a 532 nm laser. a) Cy3B, b) Atto550, c) Atto565, d) AttoRho6G, e) Alexa532 and f) Atto532 with e), f) 6 µW, a), d) 12 µW and b), c) 24 µW laser excitation power at 532 nm and a repetition rate of 20 MHz. Time resolution (= analysis period t_{acq}) of 500 ms for a)–d) and 2.5 s for e) and f). CoPS estimates correlate with intensity bleaching steps. Label number estimates with error bars derived from resampling algorithm (black), intensity (black).

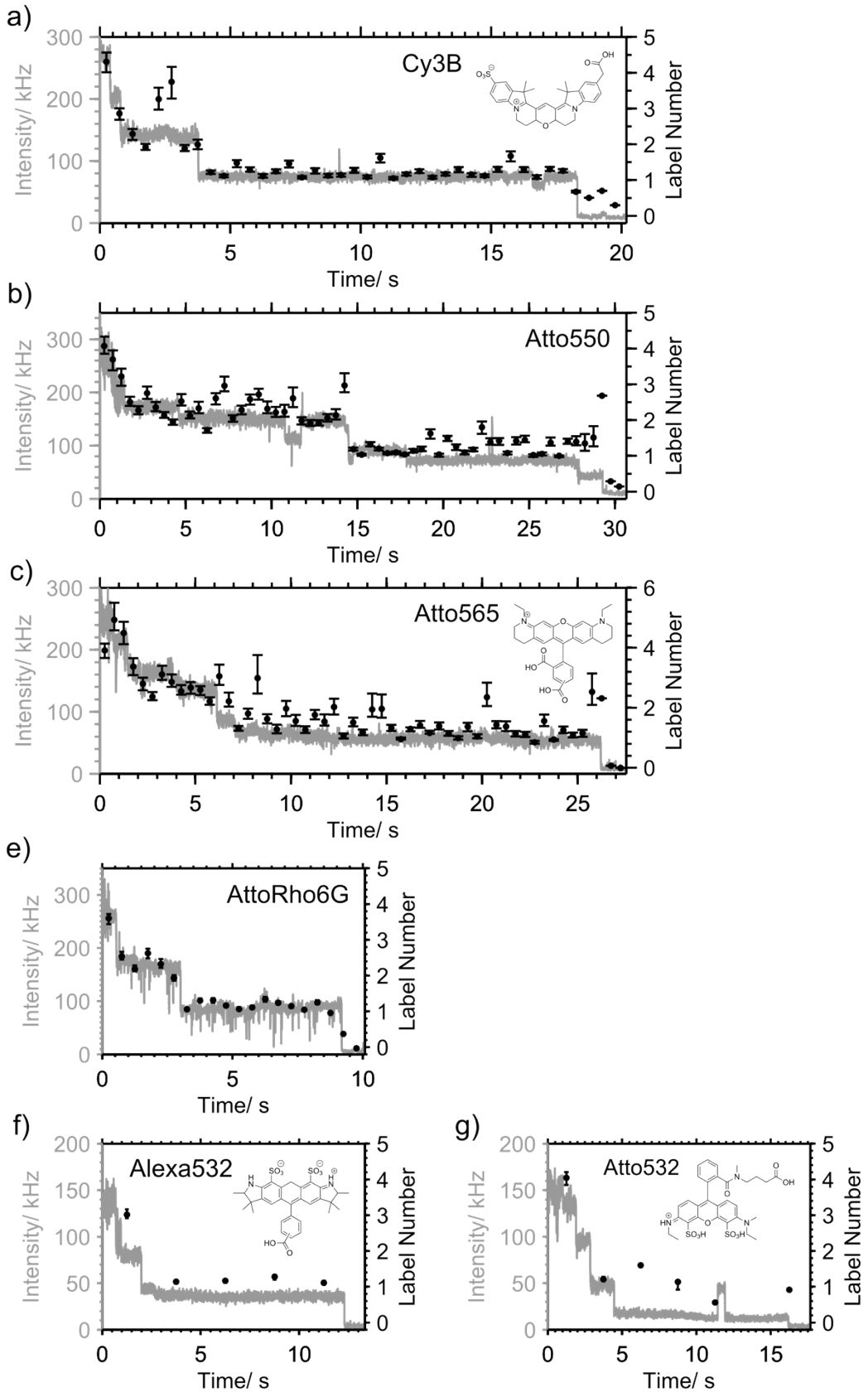
a)
Cy3B
Intensity/ kHz
Label Number
Time/ s
b)
Atto550
Intensity/ kHz
Label Number
Time/ s
c)
Atto565
Intensity/ kHz
Label Number
Time/ s
e)
AttoRho6G
Intensity/ kHz
Label Number
Time/ s
f)
Alexa532
Intensity/ kHz
Label Number
Time/ s
g)
Atto532
Intensity/ kHz
Label Number
Time/ s

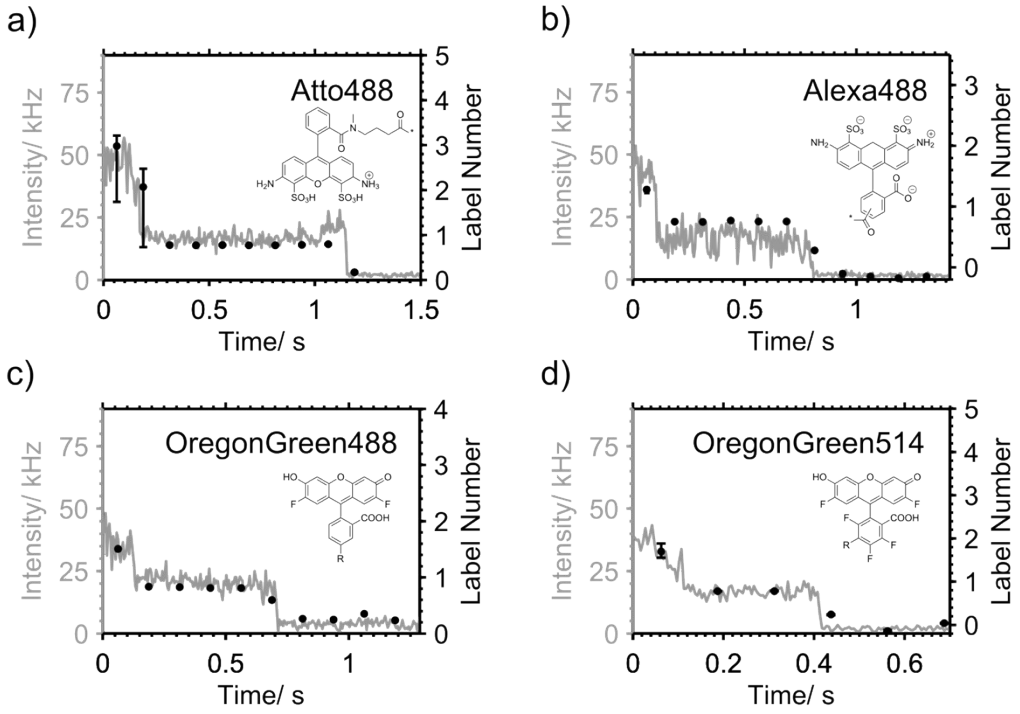

Figure S15. Single molecule CoPS analysis of DNA hybridization probe labeled with dyes that are excited with a 470 nm laser. a) Atto488, b) Alexa488, c) OregonGreen488 and d) OregonGreen514 at 6.75 µW laser excitation power at 470 nm and a repetition rate of 20 MHz. Time resolution (= analysis period t_{acq}) of 125 ms. CoPS estimates correlate with intensity bleaching steps. Traces are not representative; most dyes photobleached faster. Label number estimates with error bars derived from resampling algorithm (black), intensity (grey).

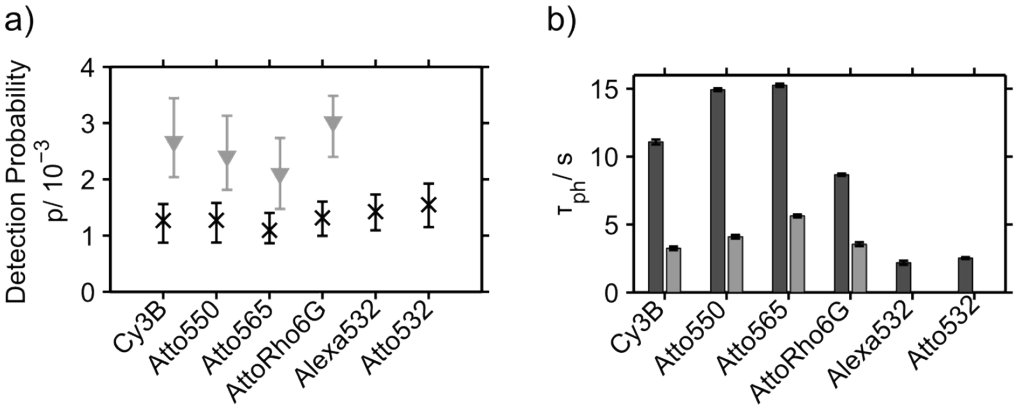

Figure S16. Single molecule CoPS analysis of DNA hybridization probe labeled with dyes that are excited with a 532 nm laser. Black crosses/ light grey downward-pointing triangles: low and high laser excitation power (6µW and 12µW for Cy3B, AttoRho6G, Alexa532 and Atto532, 12µW and 24µW for Atto550 and Atto565) at 532nm and a repetition rate of 20 MHz. a) Estimated detection probabilities (median with $Q_{0.25}$ and $Q_{0.75}$) for CoPS analysis with t_{acq} = 500 ms for low and t_{acq}= 125 ms for high laser excitation power. b) Average photostability lifetime τ_{ph} estimated by fitting a single-exponential decay to photostability time histograms derived from fluorescent traces. Errors indicate the 95% confidence intervals of the fit parameter τ_{ph}.

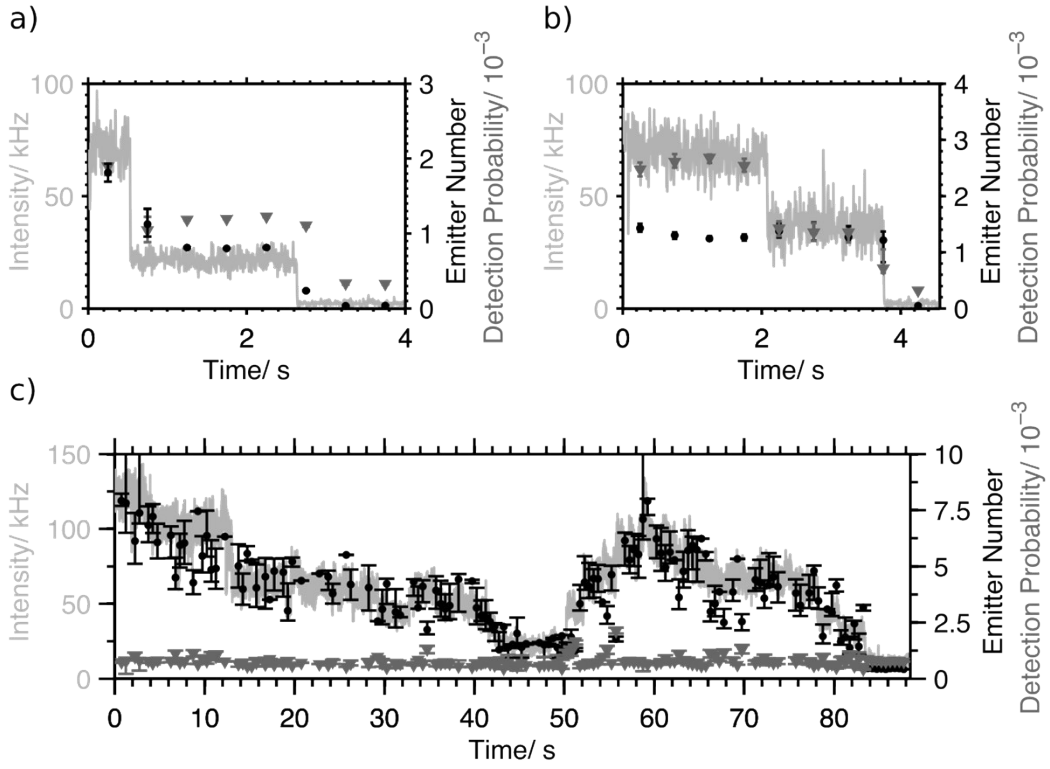

Figure S17. Time-resolved photon statistics analysis of photophysical dynamics in proteins and conjugated polymers. Fluorescence intensity (light grey), emitter number (black dots) and detection probability (dark grey downward-pointing triangles) estimates with 500 ms time resolution and errors determined by resampling. Labeled streptavidin-Alexa647 with a step in the intensity transient due to a) photobleaching of one emitter or b) changing brightness of one emitter. Experimental conditions were 5µW laser excitation power at 635 nm and a repetition rate of 20 MHz. c) Changing number of independent emitters in a single, 55 kDa poly(3-hexylthiophene) (P3HT) chain in Zeonex due to temporary quenching by deep charge trap states at about 45s followed by photodestruction[2] after about 80s. Experimental conditions were 2 µW laser excitation power at 470 nm and a repetition rate of 20 MHz.

References

1 K. S. Grußmayer, A. Kurz and D.-P. Herten, *ChemPhysChem*, 2014, **15**, 734–742.

2 K. S. Grußmayer, F. Steiner, J. M. Lupton, D.-P. Herten and J. Vogelsang, *ChemPhysChem*, 2015, **16**, 3578–3583.